UNCERTAINTY ANALYSIS FOR EXPERIMENTAL HEAT TRANSFER DATA OBTAINED BY THE WILSON PLOT METHOD
Application to condensation on horizontal plain tubes

by

Francisco J. UHIA [a], Antonio CAMPO [b], and Jose FERNANDEZ-SEARA [a]*

[a] Area de Maquinas y Motores Termicos, E.T.S. de Ingenieros Industriales, Universidad de Vigo, Vigo, Spain
[b] Department of Mechanical Engineering, The University of Texas at San Antonio, San Antonio, Tex., USA

Original scientific paper
DOI: 10.2298/TSCI110701136U

The accurate estimation of convection coefficients constitutes a crucial issue in designing and sizing any type of heat exchange device. The Wilson plot method and its subsequent modifications deliver a suitable procedure to estimate the convection coefficients from the post-processing of experimental data in a multitude of convective heat transfer processes. Uncertainty analysis is a powerful tool not only for handling the data and reporting coherent results of a certain experimental program, but also is a valuable tool in those stages devoted to the experimental design. This paper details the application of an analytical methodology for calculating the uncertainty associated with experimental data obtained by the Wilson plot method. Results based on a representative Wilson plot experiment to measure the condensation coefficients of R-134a over a horizontal 19 mm diameter smooth tube are shown. A parametric analysis was carried out sequentially to investigate the influence of the uncertainties in the measured variables and design parameters of the Wilson plot experiment in the results uncertainties. Although the example presented in this paper relates to a specific heat transfer process, the technique turns out to be rather general and can be extended to any heat transfer problem.

Key words: *uncertainty analysis, Wilson plot method, condensation, R-134a*

Introduction

Experimental programs are needed in science and technology to demonstrate physical principles and to validate processes or systems whenever analytical procedures are not feasible or are complicated. Experimental results are subjected to certain errors that emanate from various sources, such as instrumentation inaccuracies, measurement techniques, limitations in the experimental facilities, environmental variability, and so on. Conceptually, the term error defines the deviation between the experimental result and the true value. The true value is generally unknown, and as a consequence, the error of the experimental measurement cannot be determined. Because this information is crucial to establish the validity of any experimental result, a consistent method must be developed to estimate the experimental error. The concept of uncertainty is used to quantify the degree of goodness of the experimental result and has been traditionally considered as the best estimate of the experimental error.

In many cases, the experimental measurements cannot be done directly. Instead, the experimental results are methodically obtained through a data reduction procedure involving

* Corresponding author; e-mail: jseara@uvigo.es

one or more data reduction equations from several input variables. These input variables are measured experimentally and/or are obtainable from publications in the archival literature. In these cases, the simplest available approach to quantify the uncertainty in the experimental results is to perform multi-sample experiments. In the case of multi-sample experiments, the quantity of interest must be measured repeatedly under the same conditions, using different measuring instruments and experimental equipment by means of multiple observers. Thereafter, the uncertainty in the results caused by all possible uncertainty sources can be estimated by statistical parameters of the experimental measurements. Unfortunately, this type of approach is unfeasible in most experimental programs mostly due to the salaries of technical personnel, cost of equipment and time spent.

Owing to these obstacles, in practical situations, single-sample experiments are preferable. In single-sample experiments, the uncertainty in the results cannot be determined by statistical analysis and it must be evaluated from the uncertainties in the input variables. To estimate the uncertainty in the final results, the methodology associated with the propagation of the uncertainties in the input variables through the data reduction equations is the well-known uncertainty analysis. Therefore, the uncertainty analysis provides a useful tool to the analyst to understand the behaviour of the uncertainty in each input variable through the data reduction equations. Besides, uncertainty analysis brings forward a better knowledge of the step-by-step measurement process.

Further, uncertainty analysis is a powerful tool not only in the early stages of data analysis and the latter stages of the presentation of the results, but also during the design phase of the experiments. In this phase, this type of analysis can be used to identify the variables that will exert greatest influence on the results uncertainty and to investigate how accurately a magnitude could be determined from the input variables with given levels of uncertainties. On the other hand, the uncertainty analysis also enables the analyst to evaluate the measurement uncertainties needed in the input variables to ultimately obtain a desired uncertainty in the results. Finally, if several data reduction procedures are available, the uncertainty analysis can be helpful in the selection of the best alternative from the standpoint of providing the least uncertainty in the results. Based on the above-mentioned reasons, it is clear that the uncertainty analysis should be performed in the initial stage of any experimental program with a goal at improving the experiments design. This early analysis is beneficial because on one hand it can avoid unsatisfactory results and on the other hand it contributes to time and money savings.

Devised originally by Wilson [1], the Wilson plot method constitutes a robust technique to estimate the convection coefficients in a wide spectrum of convective heat transfer processes. The Wilson plot method is based on the separation of the overall thermal resistance from appropriate experimental data by means of a linear regression analysis. In the last century, the Wilson plot method along with its subsequent modifications attributed primarily to Briggs and Young [2], Shah [3], Khartabil and Christensen [4], and Khartabil *et al.* [5] became popular for the determination of heat transfer experimental data in the area of heat exchangers and heat transfer processes. In a recent state-of-the-art review paper Fernandez-Seara *et al.* [6] compiled the salient modifications of the Wilson plot method that have been divulged in the specialized literature. These authors gathered representative articles that revolved on the use of the Wilson plot method to procure experimental heat transfer data in numerous applications of heat transfer engineering.

It is worth noting that a variety of the experimental heat transfer coefficients reported in the scientific literature have been obtained by data reduction procedures based on the Wilson plot method, but unfortunately the uncertainties linked to the results are usually lacking. Repre-

sentative publications of this effort are those by Singh *et al*. [7], Yang and Chiang [8], Rennie and Raghavan [9], Kumar *et al*. [10], and Xiaowen and Lee [11]. Only a few papers such as Wojs and Tietze [12], Styrylska and Lechowska [13], Rose [14], or Cheng and Tao [15] touched upon the accuracy of the Wilson plot technique. Wojs and Tietze [12] reported an interesting analysis on the implications of the accuracy of the measured temperatures to apply the Wilson plot method. The authors insisted on the importance of making use of adequate experimental data to obtain useful results. Styrylska and Lechowska [13] purported a unified Wilson plot method for heat exchangers for conditions wherein a Nusselt equation is tied up to one of the fluids if the other does not suffer a phase change. This proposal is potent because it permits the calculation of any number of unknown constants, treating the unknowns as observations with a covariance matrix known a priori. Rose [14] proposed to compute the third unknown constant by way of an iterative scheme resulting from the minimization of the sum of squares of the residuals of the overall temperature difference in order to improve the results accuracy provided by the Wilson plot method. Cheng and Tao [15] applied the Nusselt model for condensing R-152a on horizontal tubes and found it to be accurate within 15% for a constant value of 0.725. The authors pointed out that the accuracy of the inner heat transfer coefficient (HTC) should be taken into account in the data reduction procedure.

The Wilson plot techniques involve a linear regression analysis which makes the uncertainty analysis more tedious than the calculation of the HTC. Therefore, the estimation of the uncertainties associated with the experimental results is usually overlooked. However, experimental results are not fully understood without mentioning the uncertainty associated to them. Incidentally, the uncertainties facilitate useful information to compare experimental data from different sources and of equal importance to validate mathematical models against experimental data.

This paper details the application of an analytical methodology for calculating the uncertainty associated with experimental data obtained by the Wilson plot method. The Wilson plot method is applied to the specific case of the R134a condensation on a 19 mm diameter horizontal smooth tube using water flowing inside the tube as the cooling medium. The results will elucidate and discuss the influence of the uncertainties in the measured variables and design parameters of the experiment in the results uncertainties.

General Wilson plot technique

The Wilson plot method originally proposed by Wilson [1] in 1915 was envisioned to evaluate the convection coefficients in shell and tube condensers for the case of vapour condensing outside by means of cold water flowing inside. Later on, modifications of the Wilson plot method were geared at other types of heat transfer processes and heat exchanger devices. In the following paragraphs, a general data reduction procedure based on the Wilson plot method will be delineated.

Fundamentally, in a shell and tube condenser, the overall thermal resistance of the global heat transfer process can be expressed as the sum of three partial thermal resistances corresponding to inner convection, conduction through the tube wall and outer convection. For simplicity, the thermal resistances due to the fluid fouling can be safely neglected when experiments are designed to obtain experimental data of a given convection problem. Therefore, the internal and external fouling resistances are not accounted for in the analysis, as indicated in eq. (1):

$$R_{ov} = R_i + R_t + R_o \tag{1}$$

Employing the proper expressions for each individual thermal resistance, the convective thermal resistances can be expressed as a function of the inner and the outer heat transfer ar-

eas, the inner and outer HTC and the thermal resistance of the tube wall, as indicated in eq. (2). For other two-fluid heat exchangers, eqs. (1) and (2) can be expressed as a function of thermal resistances of the cold fluid convection, the separating wall and the hot fluid convection:

$$R_{ov} = \frac{1}{h_i A_i} + R_t \frac{1}{h_o A_o} \tag{2}$$

The Wilson plot method under study here rests on the assumption of suitable functional forms of the HTC for the convection processes that occur inside and outside the tube. This task is accomplished by considering appropriate models for predicting the variation of both HTC within the experimental conditions tested, including an unknown multiplier to fit the model predictions to the experimental data. Under these assumptions, the inner and outer HTC can be expressed by eqs. (3) and (4), where h_i^* and h_o^* represent the assumed variation HTC models and C_i and C_o denote the correcting constants:

$$h_i = C_i h_i^* \tag{3}$$

$$h_o = C_o h_o^* \tag{4}$$

Substituting eqs. (3) and (4) into eq. (2) and operating, the overall thermal resistance equation can be rearranged into a linear functional form $y = ax + b$ as indicated in eq. (5). In eq. (5), the subscripts i and o are interchangeable depending on the nature of the heat transfer process and the design of the experiments:

$$(R_{ov} - R_t)h_o^* A_o = \frac{1}{C_i}\frac{h_o^*}{h_i^*}\frac{A_o}{A_i} + \frac{1}{C_o} \tag{5}$$

In harmony with this equation, experimental y-values can be represented on an x-y plane, *i. e.* the so-called Wilson plot, as a function of the experimental x-values at different operating conditions. Thereafter, the straight-line equation that fits the experimental data can be deduced by applying a linear regression. Consequently, the slope a and the intercept b from the straight line are determined. At the end, the inner and outer HTC can be calculated from eqs. (3) and (4), respectively. Figure 1 illustrates the construction of a Wilson plot based on the structure of eq. (5).

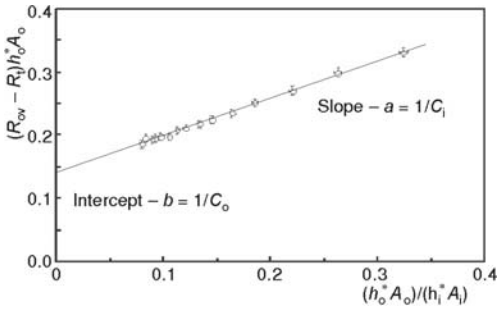

Figure 1. Wilson plot in concordance with eq. (5)

In order to obtain accurate results, the experiments must be designed to generate a large collection of x-values and y-values. In turn, this is usually accomplished by varying the flow rate of one of the fluids to obtain a large variation in the HTC. This is linked to a wide range of x-values, while keeping the HTC of the other fluid as higher as possible to a large variation in the overall thermal resistance, *i. e.*, a wide range of y-values.

Uncertainty analysis

The Wilson plot method is systematically implemented to estimate experimental convection HTC of a certain heat transfer process of interest. As noted in *General Wilson plot technique*, the experimental HTC are calculated from several measured variables by means of a data reduction procedure involving several simple equations. The uncertainties in the measured vari-

ables propagate through the data reduction equations to the final set of results. Therefore, these results should be articulated with their associated uncertainties to instil greater consistence to the results. The uncertainties in the results should be carefully analysed because they provide useful information about the reliability of the results and the entire measurement process.

In this section, a systematic calculation procedure is proposed to evaluate the uncertainty in the HTC obtained by the Wilson plot method. The analysis is based on the application of the general uncertainty propagation expression given by eq. (6) and taken from ISO [16]. In eq. (6), u stands for the standard uncertainty, which is equivalent to the standard deviation, and v_j stands for the variables that contribute to the uncertainty in the result r that revolves around any data reduction equation. In the analysis, the uncertainties in the input variables are assumed to be uncorrelated. As a result, the covariance terms in eq. (6) are neglected:

$$u(r) = \sqrt{\sum_{j=1}^{n}\left[\frac{\partial r}{\partial v_j}u(v_j)\right]^2} \tag{6}$$

By way of illustration, the specific process of condensation of R-134a on a horizontal smooth tube is undertaken. With regards to the cooling medium, water circulates inside the tube with a fully developed turbulent velocity. The Wilson plot method is used as a data reduction technique to determine first the vapour condensation HTC on the outer surface of the tube and second the inner convection coefficients inside the tube. An experimental facility is needed to perform the condensation process within the framework of the experimental program envisioned. Careful experiments have to be designed and later conducted to measure the vapour condensation temperature T_{v}, the cooling water inlet temperature T_{cwi}, and the cooling water outlet temperature T_{cwo} at various cooling water mass flow rates ($\dot{m}_{\mathrm{cw}}$), that are also measured.

The variables subjected to various levels of error are the measured quantities. The uncertainty in the results due to tolerances in geometrical parameters of the tube and the uncertainties in the estimation of the fluid properties and tube material properties were previously tested. Owing that the group of parameters and properties represent less than 1% of the final uncertainty in the results, for the sake of simplicity, they are not considered in the analysis.

The data reduction procedure for the Wilson plot method necessitates the determination of the internal and external areas of the tube, the tube wall thermal resistance, the overall thermal resistance and the adequate assumption of the functional forms for the inner and outer HTC, according to eq. (5). The inner/outer areas of the tube are determined from eq. (7) as a function of the inner/outer tube diameter and the tube length. The tube wall thermal resistance is computed from eq. (8):

$$A_{\mathrm{i/o}} = \pi d_{\mathrm{i/o}} L_{\mathrm{t}} \tag{7}$$

$$R_{\mathrm{t}} = \frac{\ln\dfrac{d_o}{d_i}}{2\pi k_{\mathrm{t}} L_{\mathrm{t}}} \tag{8}$$

The variables participating in the preceding eqs. (7) and (8) are not subjected to uncertainty. In this regard, the areas of the tube as well as the wall thermal resistance are obtained with zero uncertainty.

The overall thermal resistance is calculated with eq. (9). In this equation, the ΔT_{lm} is the logarithmic mean temperature difference and q_{cw} – the heat transfer rate. The logarithmic mean temperature difference is calculated from the inlet and outlet water temperatures and the vapour condensing temperature according to eq. (10).

$$R_{ov} = \frac{\Delta T_{lm}}{q_{cw}} \tag{9}$$

$$\Delta T_{lm} = \frac{(T_v - T_{cwi}) - (T_v - T_{cwo})}{\ln \dfrac{T_v - T_{cwi}}{T_v - T_{cwo}}} \tag{10}$$

The heat transfer rate is determined from an energy balance in the cooling water given by eq. {11) as a function of the mass flow rate, the specific heat capacity and the inlet and outlet temperature difference:

$$q_{cw} = \dot{m}_{cw} C_{pcw} (T_{cwo} - T_{cwi}) \tag{11}$$

The input variables in the pair of eqs. (10) and (11) along with their associated uncertainties are the inlet and outlet cooling water temperatures, the condensing vapour temperature and the cooling water mass flow rate. Following eq. (6), the uncertainties in the logarithmic mean temperature difference and in the heat transfer flow rate are found from eqs. (12) and (13), respectively:

$$u(\Delta T_{lm}) = \sqrt{\left[\frac{\partial \Delta T_{lm}}{\partial T_v} u(T_v)\right]^2 + \left[\frac{\partial \Delta T_{lm}}{\partial T_{cwi}} u(T_{cwi})\right]^2 + \left[\frac{\partial \Delta T_{lm}}{\partial T_{cwo}} u(T_{cwo})\right]^2} \tag{12}$$

$$u(q_{cw}) = \sqrt{\left[\frac{\partial q_{lm}}{\partial \dot{m}_{cw}} u(\dot{m}_{cw})\right]^2 + \left[\frac{\partial q_{cw}}{\partial T_{cwi}} u(T_{cwi})\right]^2 + \left[\frac{\partial q_{cw}}{\partial T_{cw}} u(T_{cwo})\right]^2} \tag{13}$$

Once the uncertainties in the logarithmic mean temperature difference and in the heat transfer flow rate are established, the uncertainty in the overall thermal resistance can be calculated from eq. (14):

$$u(R_{ov}) = \sqrt{\left[\frac{\partial R_{ov}}{\partial \Delta T_{lm}} u(\Delta_{lm})\right]^2 + \left[\frac{\partial R_{ov}}{\partial q_{cw}} u(q_{cw})\right]^2} \tag{14}$$

As stated before, the cooling water circulates inside the tube with fully developed turbulent velocity ($Re_{cw} \geq 10{,}000$). For this high velocity, the convection HTC in a circular smooth tube is proportional to $Re_{cw}^{4/5}$, according to Colburn [17]. Moreover, if the fluid bulk temperature is maintained nearly constant during the experiment, the influence exerted by the variation of the liquid flow rate on the fluid properties is negligible. Then, under this assumption, the variation of the internal HTC can be modelled by eq. (15), where the cooling water Reynolds number is given by eq. (16):

$$h_i^* = \sqrt[5]{Re_{cw}^4} \tag{15}$$

$$Re_{cw} = \frac{4\dot{m}_{cw}}{\mu_{cw}} \tag{16}$$

Inspecting eq. (16), it is clear that the water flow rate is the only contributor to the uncertainty in the water Reynolds number. As a consequence, the uncertainty in the Reynolds number is expressed by eq. (17) and the uncertainty in h_i^* is expressed by eq. (18):

$$u(Re_{cw}) = \frac{\partial Re_{cw}}{\partial \dot{m}_{cw}} u(\dot{m}_{cw}) \tag{17}$$

$$u(h_i^*) = \frac{\partial h_i^*}{\partial \mathrm{Re}_{\mathrm{cw}}} u(\mathrm{Re}_{\mathrm{cw}}) \tag{18}$$

According to the Nusselt theory [18], the variations of the outside HTC at different operating conditions are mainly due to the variations of the liquid film thickness over the external surface of the tube. For a nearly constant vapour temperature, the effects of the condensate properties in the condensate film thickness are unimportant and the condensation HTC can be considered to be proportional to the condensate Reynolds number. Thus, on base of the Nusselt equation and under the assumption of constant vapour temperature eq. (19) is considered as variation model to the outside HTC.

$$h_o^* = \frac{1}{\sqrt[3]{\mathrm{Re}_{\mathrm{c}}}} \tag{19}$$

Herein, the condensate Reynolds number is defined by eq. (20), where the condensate flow rate is determined from the heat transfer flow rate together with the latent heat of the condensing vapour from eq. (21):

$$\mathrm{Re}_{\mathrm{c}} = \frac{2\dot{m}_{\mathrm{c}}}{\mu_{\mathrm{c}} L_{\mathrm{t}}} \tag{20}$$

$$\dot{m}_{\mathrm{c}} = \frac{q_{\mathrm{cw}}}{\lambda} \tag{21}$$

The uncertainty in the condensate Reynolds number takes into account the uncertainty in the heat transfer flow rate according to eq. (22). In addition, the uncertainty in the condensate Reynolds number is calculated from eq. (23):

$$u(m_{\mathrm{c}}) = \frac{\partial m_{\mathrm{c}}}{\partial q_{\mathrm{cw}}} u(q_{\mathrm{cw}}) \tag{22}$$

$$u(\mathrm{Re}_{\mathrm{c}}) = \frac{\partial \mathrm{Re}_{\mathrm{c}}}{\partial \dot{m}_{\mathrm{c}}} u(\dot{m}_{\mathrm{c}}) \tag{23}$$

Finally, the uncertainty in h_{o}^* can be extracted from eq. (24) as a function of the uncertainty in the condensate Reynolds number.

$$u(h_{\mathrm{o}}^*) = \frac{\partial h_{\mathrm{o}}^*}{\partial \mathrm{Re}_{\mathrm{c}}} u(\mathrm{Re}_{\mathrm{c}}) \tag{24}$$

The y-axis and x-axis Wilson plot values are represented by the tandem of eqs. (25) and (26):

$$y = (R_{\mathrm{ov}} - R_{\mathrm{t}}) h_{\mathrm{o}}^* A_{\mathrm{o}} \tag{25}$$

$$x = \frac{h_{\mathrm{o}}^* A_{\mathrm{o}}}{h_{\mathrm{i}}^* A_{\mathrm{i}}} \tag{26}$$

The information for the inner and outer tube areas comes from eq. (7), the tube wall thermal resistance from eq. (8), the overall thermal resistance from eq. (9), and the inner and outer HTC variation models from eqs. (15) and (19), respectively.

The input variables along with their associated uncertainties in eq. (25) are the overall thermal resistance and the outer HTC variation model. As a result, the uncertainty in the y-axis Wilson plot values are derived from eq. (27):

$$u(y) = \sqrt{\left[\frac{\partial y}{\partial R_{\mathrm{ov}}} u(R_{\mathrm{ov}})\right]^2 + \left[\frac{\partial y}{\partial h_{\mathrm{o}}^*} u(h_{\mathrm{o}}^*)\right]^2} \tag{27}$$

On the other hand, the input variables subject to uncertainties in eq. (26) are the inner and outer HTC variation models. Consequently, the uncertainty in the x-axis Wilson plot values are calculated from eq. (28):

$$u(x) = \sqrt{\left[\frac{\partial x}{\partial h_{\mathrm{o}}^*}\,u(h_{\mathrm{o}}^*)\right]^2 + \left[\frac{\partial x}{\partial h_{\mathrm{i}}^*}\,u(h_{\mathrm{i}}^*)\right]^2} \tag{28}$$

In view of the foregoing statements, the experimental y-values can be plotted against the experimental x-values at several operating conditions (*i. e.*, water flow rates) on a typical Wilson plot. Hence, the equation of the straight line $y = ax + b$ that best correlates the experimental data can be estimated by means of regression analysis. To calculate the accurate values of the slope a and the intercept b, it is necessary to realize that not all the data points usually share the same degree of uncertainty. In this sense, the data with low uncertainty should have a greater influence on the fitting parameters than the data with high uncertainty. This issue is appropriately tackled by applying the weighted least squared (WLS), method which consists in finding the fitting parameters that minimize the Chi-squared function (χ^2). For the specific case of a linear model, the Chi-squared function is given by eq. (29). In this equation u_j identifies the standard uncertainty associated to the data pair $(x, y)_j$, and the quantity $1/u_j^2$ is a weighting factor:

$$\chi^2 = \sum_{j=1}^{n} \frac{(y_j - ax_j - b)^2}{u_j^2} \tag{29}$$

When applying the Wilson method the most widespread procedure discards the effect of the uncertainty in the independent variable – $u(x_j) = 0$, *i. e.*, only the measurement uncertainty in the dependent variable is taken into account ($u_j = u(y_j)$). Unfortunately, in many cases, the measurement uncertainties in both variables share the same order of magnitude and the contribution to the uncertainty of the x-axis values should not be neglected (Bevington and Robinson [18]). Under these broader circumstances, a more general WLS method must be employed to incorporate the contributions of the x-values and y-values uncertainties toward the total uncertainty of each data pair, as indicated in eq. (30). Thereby, the task of fitting the straight line model turns out to be more difficulty due to the presence of the parameter a in the denominator of the Chi-squared function:

$$u_j = \sqrt{\{[u(y)]^2 + [au(x)]^2\}_j} \tag{30}$$

Upon differentiating the Chi-squared function with respect to a and b, setting the derivatives equal to zero and rearranging the resulting equations, explicit expressions to calculate the slope a and the intercept b of the linear model are obtained. This is quantified by the tandem of eqs. (31) and (32):

$$a = \frac{\sum_{j=1}^{n}\frac{1}{u_j^2}\sum_{j=1}^{n}\frac{x_j y_j}{u_j^2} - \sum_{j=1}^{n}\frac{x_j}{u_j^2}\sum_{j=1}^{n}\frac{y_j}{u_j^2}}{\sum_{j=1}^{n}\frac{1}{u_j^2}\sum_{j=1}^{n}\frac{x_j^2}{u_j^2} - \left(\sum_{j=1}^{n}\frac{x_j}{u_j^2}\right)^2} \tag{31}$$

$$b = \frac{\sum_{j=1}^{n}\frac{x_j^2}{u_j^2}\sum_{j=1}^{n}\frac{x_j}{u_j^2} - \sum_{j=1}^{n}\frac{x_j}{u_j^2}\sum_{j=1}^{n}\frac{x_j y_j}{u_j^2}}{\sum_{j=1}^{n}\frac{1}{u_j^2}\sum_{j=1}^{n}\frac{x_j^2}{u_j^2} - \left(\sum_{j=1}^{n}\frac{x_j}{u_j^2}\right)^2} \tag{32}$$

As can be extracted from eqs. (29), (30), and (31), the equation for the slope in the WLS method absorbing the two uncertainties in both x-values and y-values is non-linear. Therefore, an iterative procedure is forcibly needed. The simplest procedure consists in the following steps:

– assumption of a starting value of a in eq. (29),
– calculation of the uncertainty in each data pair from eq. (30), and
– determination of a revised value of a from eq. (31) until the difference between the assumed and calculated values satisfy a desired pre-set accuracy.

Upon applying the general uncertainty propagation expression to eqs. (31) and (32) and taking into account the uncertainty associated to each data pair (u_j), eqs. (33) and (34) emerged to calculate the uncertainties in a and b, respectively:

$$u(a) = \sqrt{\sum_{j=1}^{n}\left(\frac{\partial a}{\partial y_j}u_j\right)^2} \tag{33}$$

$$u(b) = \sqrt{\sum_{j=1}^{n}\left(\frac{\partial b}{\partial y_j}u_j\right)^2} \tag{34}$$

After doing the algebra and re-arranging terms, eqs. (33) and (34) can be channeled as functions of the Wilson plot x-values and the uncertainties of each data pair. In equation form, this corresponds to eqs. (35) and (36):

$$u(a) = \sqrt{\frac{\sum_{j=1}^{n}\frac{1}{u_j^2}}{\sum_{j=1}^{n}\frac{1}{u_j^2}\sum_{j=1}^{n}\frac{x_j^2}{u_j^2} - \left(\sum_{j=1}^{n}\frac{x_j}{u_j^2}\right)^2}} \tag{35}$$

$$u(b) = \sqrt{\frac{\sum_{j=1}^{n}\frac{x_j^2}{u_j^2}}{\sum_{j=1}^{n}\frac{1}{u_j^2}\sum_{j=1}^{n}\frac{x_j^2}{u_j^2} - \left(\sum_{j=1}^{n}\frac{x_j}{u_j^2}\right)^2}} \tag{36}$$

Once the fitting parameters a and b are determined, the constants C_i and C_o can be calculated from eqs. (37) and (38), as can be extracted from eq. (5):

$$C_\mathrm{i} = \frac{1}{a} \tag{37}$$

$$C_\mathrm{o} = \frac{1}{b} \tag{38}$$

Thereafter, the uncertainties in the constants C_i and C_o are calculated from eqs. (39) and (40), as a function of the uncertainties in a and b:

$$u(C_\mathrm{i}) = \frac{\partial C_\mathrm{i}}{\partial a}u(a) \tag{39}$$

$$u(C_o) = \frac{\partial C_o}{\partial b} u(b) \tag{40}$$

The final values of the inner and outer HTC are calculated from the HTC variation models h_i^* and h_e^* and the correcting constants C_i and C_o, according to the assumed functional forms in eqs. (3) and (4), respectively. Therefore, the uncertainties in final inner and outer HTC, h_i, and h_o, are given by eqs. (41) and (42).

$$u(h_i) = \sqrt{\left[\frac{\partial h_i}{\partial h_i^*} u(h_i^*)\right]^2 \left[\frac{\partial h_i}{\partial C_i} u(C_i)\right]^2} \tag{41}$$

$$u(h_o) = \sqrt{\left[\frac{\partial h_o}{\partial h_o^*} u(h_o^*)\right]^2 \left[\frac{\partial h_o}{\partial C_o} u(C_o)\right]^2} \tag{42}$$

The standard uncertainty obtained by eqs. (41) and (42) implies that the true value is expected to lie within the band $\pm u(r)$ around the measured value with an embedded 68.3% confidence level. However, the most widely used procedure is to express the uncertainty of results with 95% confidence level. The uncertainty with a 95% confidence level (U), or expanded uncertainty, is related with the standard uncertainty (u) by means a coverage factor (CF), as indicated in eqs. (43) and (44). Herein, CF = 2 is the recommended value for the CF to give rise to the 95% confidence interval assuming a normal distribution in the experimental results, h_i and h_o. Finally, the relative uncertainties are given by the ratio of the standard/expanded uncertainty to the size measured value:

$$U(h_i) = \mathrm{CF}u(h_i) \tag{43}$$

$$U(h_o) = \mathrm{CF}u(h_o) \tag{44}$$

The uncertainty calculation procedure presented in this section enables us to estimate the uncertainty in the inner and the outer HTC when the Wilson plot technique is used to obtain experimental data of a heat transfer process consisting on a pure fluid vapour condensing on a horizontal tube internally cooled by a turbulent liquid flow. Although the example reported in the present paper is focused on a specific heat transfer process, it can be easily extended to other heat transfer processes by taking into account the appropriate HTC variation models (h^*) for the specific convection processes under consideration.

Presentation of results

Unquestionably, the Wilson plot method provides a logical framework to evaluate the condensation HTC of R-134a vapour on a horizontal smooth tube internally cooled by water. The calculation procedure exposed in the section Uncertainty analysis was applied to investigate how the uncertainties in the measured variables propagate through the data reduction equations and ultimately to the results. The geometry and material properties of the tube under consideration in the analysis are listed in tab. 1 and the prevalent operating condition are listed in the companion tab. 2.

Table 1. Dimensions and thermal properties of the tube material

External tube diameter	19.05 mm (3/4 inch)
Tube wall thickness	1 mm
Tube length	2 m
Tube wall thermal conductivity	Copper (386 W/mK)

Firstly, the uncertainty calculation method was validated to the specific case. Secondly, the uncertainty analysis was carried out to compute the influence of the uncertainties in each input variable on the final uncertainty in the condensation HTC. Finally, the uncertainty calculation procedure was used in a parametric study to investigate the influence of the Wilson plot experiment design by varying the accuracy of input variables, the tube dimensions and operating condition in which the experimental data are taken.

Table 2. Experimental operating conditions

Condensation temperature	40 ºC
Logarithmic mean temperature difference	10 ºC
Cooling water Reynolds number variation	10,000 to 20,000
Number of measurement points	15

The input data to the Wilson plot method for the different operating conditions was computer-generated in harmony with the basic heat transfer principles. In this regard, the Dittus and Boelter [20] correlation and the Nusselt equation [18] were chosen to compute the inner and outer heat transfer coefficients, respectively. The four variables generated in this manner were the cooling water mass flow rate, the inlet water temperature, the outlet water temperature and the R-134a condensation temperature.

The uncertainties in the measured variables can be evaluated by the statistical analysis of series of observations (type A uncertainties), by any other kind of information such as the information provided by the instrumentation manufacturers or obtained from reference sources (type B uncertainties) or even by a combination of both types of data (ISO [16]) is acceptable. Understandably, the evaluation of the d ifferent sources of error necessitates knowledge of the experimental facility, the measurement instrumentation and the conditions under which the experiments was performed. For calculation purposes, the expanded uncertainties ($U_{CF=2}$) indicated in tab. 3 was considered in the analysis. The standard uncertainties (u) used as inputs to the uncertainty calculation procedure are obtained from the expanded uncertainties assuming normal distributions of the input variables. These u values are also included in tab. 3.

Table 3. Uncertainties in the measurement variables

Input vari able	$U_{CF=2}$	u
Cooling water inlet temperature	0.1 ºC	0.05 ºC
Cooling water outlet temperature	0.1 ºC	0.05 ºC
Condensation temperature	0.1 ºC	0.05 ºC
Cooling water flow rate	1% of $\dot{m}_{cw}$	0.5% of $\dot{m}_{cw}$

Validation of the uncertainty propagation model

In order to validate the uncertainty propagation model explained in the section *Uncertainty analysis*, the input data needed for the Wilson plot method was generated for the tube in tab. 1 under the operating conditions in tab. 2. Thereby, random errors within the desired uncertainty interval $\pm U(v_j)$ were introduced to the input data to simulate the intrinsic experimental measurement errors. Using these data to evaluate the convection coefficients of the heat transfer process by the Wilson plot method, the obtained values differ from those that emanate from the Dittus and Boelter [20] and Nusselt models [18], *i. e.*, the true HTC values, because of the errors introduced in the input variables. In this sense, the HTC errors can be calculated and compared against the results of the uncertainty analysis procedure exposed in *Uncertainty analysis.*

Data possessing a wide spectrum of uncertainties were sequentially tested. As a result, the true HTC values lie within the band $\pm u(h)$ in 73.5% of the cases, and only 5.5% of the cases stays outside the band $\pm U(h)$. These results convincingly demonstrate the consistency of the uncertainty propagation model presented in the section *Uncertainty analysis*. In light of this, the

results can be used with confidence to obtain information about the behaviour of the uncertainties within the platform of the Wilson plot technique.

Influence of the measurement uncertainties

The influence of the uncertainties in each input variable related to the uncertainty in the calculated R134a condensation coefficient was discussed on the basis of two normalized coefficients, the uncertainty magnification factor (*UMF*) and the uncertainty percentage contribution *UPC* (Coleman and Steele [21]).

The *UMF* is indicative of the variation of the relative uncertainty in the result due to a given variation of the relative uncertainty in each input variable. For the data reduction using simple equations, the *UMF* are usually determined by applying partial derivatives, but this approach becomes impractical for handling data reduction with complex expressions. In the present analysis, the *UMF* were evaluated using the uncertainty calculation procedure by introducing a unitary percentage uncertainty in each measured variable and setting to zero the remaining uncertainties to obtain the uncertainty variation in the condensation HTC. Correspondingly, the *UMF* are obtained from eq. (45), where $U_{r,vj}(h_o)$ represents the relative uncertainty in h_o due to the uncertainty in the input variable v_j and $U_r(v_j)$ designates the relative uncertainty in v_j. Note that the relative uncertainties of the temperature measurements were calculated in terms of absolute temperatures, as recommended by Coleman and Steele [21]:

$$UMF(v_j) = \frac{U_{r,vj}(h_o)}{U_r(v_j)} \tag{45}$$

The *UPC* defined by way of eq. (46) are indicative of the percentage contribution of the uncertainty in each input variable v_j toward the overall uncertainty in h_o. As can be observed in eq. (46), the *UPC* accounts for both the *UMF* and the uncertainty levels in the input variables by way of:

$$UPC(v_j) = \frac{UFM^2(v_j)U_r^2(v_j)}{U_r^2(h_o)}100 \tag{46}$$

The resulting relative uncertainty in the condensation HTC of R134a obtained from the experiment defined in tabs. 1 and 2 was 10.07%, taking into account the uncertainties in the input variables that appear in tab. 3. Table 4 contains the *UMF* and the *UPC* obtained for these conditions. The *UMF* in tab. 4 reveal that the cooling water inlet and the outlet temperatures are potentially the most influential input variables that contribute to the accuracy in h_o, with the mean *UMF* being around 208.8. The condensing temperature *UMF* is 9.4 times lower than the cooling water temperatures and the effect of the water flow rate becomes potentially insignificant.

Table 4. Magnitudes for the *UMF* and *UPC* of the input variables for the condensation HTC

Input variable	*UMF*	*UPC* [%]
Cooling water inlet temperature	207.2	48.2
Cooling water outlet temperature	209.0	48.2
Condensation temperature	22.2	0.6
Cooling water flow rate	1.7	3.0

Results extracted from the UMF should be corroborated by the UPC for the specific uncertainties in the input variables considered in the analysis. This aspect is related to tab 3. The

UPC values appearing in tab. 4 confirmed that the measurements of the water inlet temperature and outlet temperature are critical for the accuracy in the condensation HTC. In numbers, this is equivalent to 96.3% of the overall uncertainty in the condensation HTC. The intermediate results of the uncertainty propagation model insinuates that the dominant influence of the water temperature measurements on the final result is attributed to the large relative uncertainty in the cooling water temperature difference, namely $3.44\% \le U_r(\Delta T_{cw}) \le 8.20\%$. This unequivocally leads to a large relative uncertainty in the determination of the heat transfer flow rate ($3.58\% \le \le U_r(q_{cw}) \le 8.26\%$). These results agree with those reported by Wojs and Tietze [12] and Rose [14] who pointed out the strong influence of the uncertainty in the flowing liquid toward the results provided by the Wilson plot technique. On the other hand, the uncertainty in the water flow rate becomes the second most influential variable; this represents 3.0% of the overall uncertainty in the result. The uncertainty in the vapour temperature is the least critical input variable in the uncertainty propagation model. Obviously, this is connection to the *UPC* for the assumed input variable uncertainties.

Parametric analysis

The pair *UMF* and *UPC* depends on the specific tube geometry and the experimental operating conditions considered in the Wilson plot experiment. Thus, the *UMF* were previously calculated for each different condition considered in the parametric analysis, and then, the uncertainty in the condensation HTC and the *UPC* were obtained afterwards.

The results listed in tab. 4 clearly indicate that the measurement of the cooling water inlet/outlet temperatures are the controlling factors for the accurate determination of the condensation HTC in the experiment defined in tabs. 1 and 2. Therefore, the uncertainty in the condensation HTC could be significantly reduced by improving the accuracy in the measurements of the cooling water temperature. Figure 2 displays the relative uncertainty in the condensation HTC against the uncertainty in the water inlet/outlet temperatures keeping the remaining uncertainties in the input variables in conformity with the numbers in tab. 3. In addition, fig. 2 also included the *UPC* of the input variables. The results plotted in fig. 2 manifest that the uncertainty in the condensation HTC strongly decrease with decreasing the uncertainty in the cooling water temperature measurements. The *UPC* in fig. 2 reveal that the contribution of the water temperature measurements to the overall uncertainty in the condensation HTC strongly decrease for uncertainties under 0.1, whereas the *UPC* of the remaining input variables exponentially increase when the uncertainty in the water temperatures diminishes. It is noteworthy pointing out that for uncertainties in the water temperatures falls below 0.025, the *UPC* of the water flow rate becomes the controlling input variable in the uncertainty propagation process.

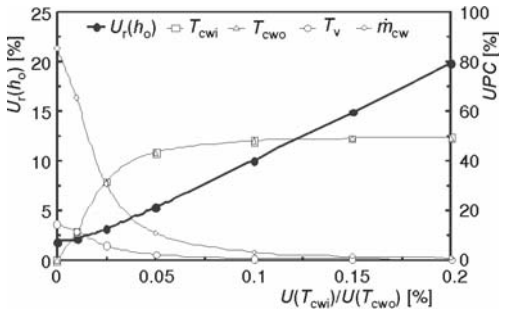

Figure 2. Uncertainty in the condensation HTC (black points) and *UPC* (white points) varying with the uncertainty in the inlet and outlet water temperatures

Figure 3 depicts the relative uncertainty in the condensation HTC and the *UPC* against the uncertainty in the water flow rate keeping the remaining uncertainties in the input variables according to the values listed in tab. 3. It is inferred from fig. 3 that the uncertainty in the condensation HTC slightly increase with increments in the uncertainty of the water flow rate. The

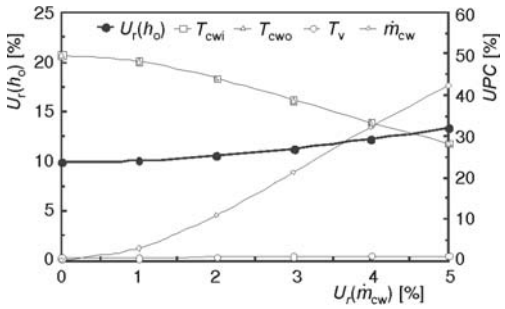

Figure 3. Uncertainty in the condensation HTC (black points) and *UPC* (white points) varying with the uncertainty in the water flow rate

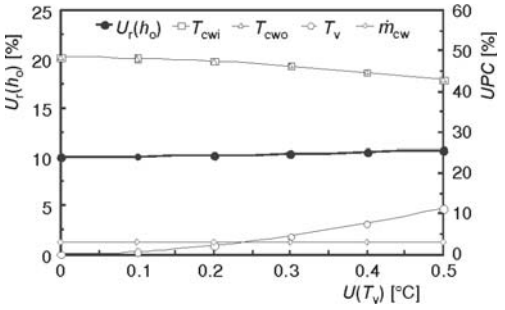

Figure 4. Uncertainty in the condensation HTC (black points) and *UPC* (white points) varying with the uncertainty in the R-134a vapour temperature

uncertainty in h_o ranges from 9.90 to 13.33 for water flow rate uncertainties from 0 to 5%. The water flow rate *UPC* increases as a result of increasing its uncertainty, becoming the controlling input variable in the uncertainty propagation model for $U_r(\dot{m}_{cw}) = 4\%$.

Shown in fig. 4 is the relative uncertainty in the condensation HTC and the *UPC* against the uncertainty in the R-134a vapour temperature keeping the remaining uncertainties in the input variables in conformity with the values listed in tab. 3. The collection of results in fig. 4 points out that the uncertainty in the condensation HTC remains nearly constant when varying the uncertainty in the vapour temperature. The uncertainty in h_o is bounded between 10.04 and 10.71 for uncertainties in the vapour temperature limited to the interval 0 to 0.5 ºC. Even when increasing the condensing temperature uncertainty up to 0.5 ºC, the companion *UPC* stays lower than 12%.

Data presented in figs. 2, 3, and 4 were generated for the tube characteristics listed in tab. 1 articulated with the operating conditions in tab. 2. Thus, UMFs remains constant and the variations of the uncertainty in h_o and its *UPC* are responsive to variations of the uncertainties in the input variables. Correspondingly, the uncertainty in the result can also be reduced by considering different Wilson plot experiment designs, *i. e.*, by diminishing the *UMF*. This task can be accomplished by considering larger tube lengths, higher logarithmic mean temperature differences (LMTD), different water Reynolds numbers or a larger number of data pairs in the platform of the Wilson plot. To illustrate this idea, the role played by the most influenced parameters in reference to the final uncertainty in the result are explained and discussed in the following subsection.

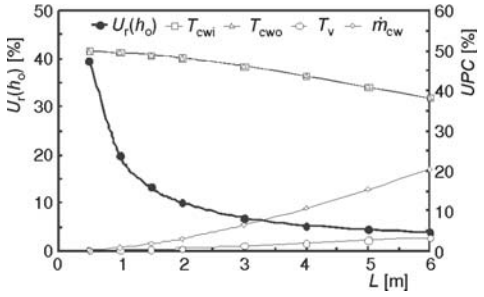

Figure 5. Uncertainties in the condensation HTC (black points) and *UPC* (white points) as a function of the tube length

As stated above, the most critical variable in the final uncertainty in the condensation HTC is the relative uncertainty in the cooling water temperature difference. The relative uncertainty in the water temperature difference can be attenuated by enlarging the LMTD or by using a larger tube length, which turn out in a higher cooling water temperature differences.

Figure 5 illustrates the relative uncertainty in the condensation HTC and its *UPC* changing

with the tube length holding constant the other tube parameters in tab. 1 and operating conditions in tab. 2. This is tied up with the input uncertainties contained in tab. 3. The numbers plotted in fig. 5 reveal that the relative uncertainty in the condensation HTC is relatively high for a tube with 0.5 m length, markedly decreases with increasing the tube length up to 2 m and slightly decreases for tube lengths greater than 2 m. The *UPC* for the inlet/outlet water temperatures decrease with enlargements of the tube length, whereas the *UPC* of the water flow rate increases with larger tubes. The *UPC* of the vapour temperature slightly increases with augmentation of the tube length and are significantly lower than the remaining *UPC* for tube lengths larger than 3 m. Therefore, the appropriate sizing of the tube length in the context of the Wilson plot experiments can contribute to the attainment of the desired accuracy of the condensation HTC.

Figure 6 contains the relative uncertainty in the condensation HTC and its *UPC* against the LMTD keeping constant the tube parameters in tab. 1 and the operating conditions in tab. 2, and engaging the input uncertainties in tab. 3. Data presented in fig. 6 show that the uncertainty in the condensation HTC decrease with increasing of the LMTD. As can be extracted from fig. 6, the augmentation of the LMTD leads to a slight decrease in the cooling water temperatures and the mass flow rate UPC, while the UPC of the vapour temperature increase by increasing the LMTD. Results contained in fig. 6 point out that the influence of the LMTD in the uncertainty of the condensation HTC is decisive for LMTD below than 10 ºC and not important for LMTD higher than 15 ºC.

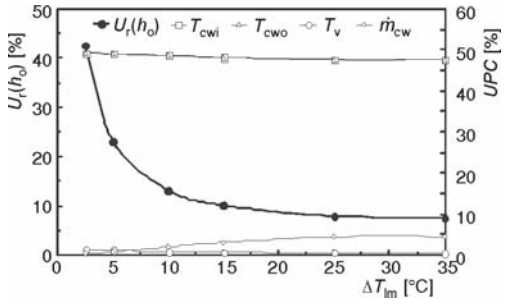

Figure 6. Uncertainties in the condensation HTC (black points) and *UPC* (white points) as a function of the logarithmic mean temperature

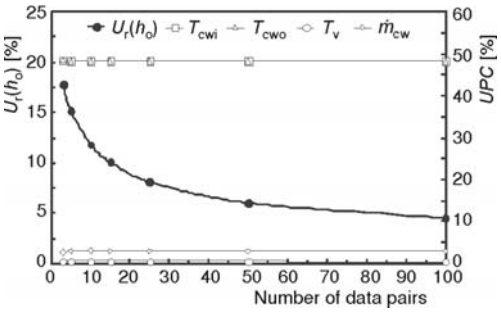

Figure 7. Uncertainties in the condensation HTC (black points) and *UPC* (white points) as a function of the number of data pairs within the Wilson plot platform

Finally, when designing an experiment, the number of different operating conditions in which measurements are made can be varied, *i. e*., the number of data pairs related to the Wilson plot. It is expected that increasing the number of data pairs engaged in the regression analysis would improve the accuracy of the regression parameters, *a* and *b*. Figure 7 displays the relative uncertainty in the condensation HTC and its *UPC* against the number of data pairs in the Wilson plot while keeping constant the remaining experimental parameters in tabs. 1 and 2, and considering the input uncertainties in tab. 3. The results plotted in fig. 7 attest that the uncertainty in the condensation HTC significantly decrease with increasing of the number of data pairs in the Wilson plot for experiments of up to 30 data pairs and slightly decrease when the number of data pairs is higher. In synthesis, the number of measurements must be taken into account in the design of Wilson plot experiments.

Conclusions

In this paper an analytical model to incorporate the uncertainty into the results obtained by the Wilson plot method has been presented. The uncertainty analysis rests primarily on the application of the general uncertainty propagation equation (ISO [16]). The uncertainty calculation procedure has been used to investigate the influence of the uncertainties in the measured variables and design parameters of the Wilson plot experiment in the condensation HTC of R-134a vapour condensing over a 19.05 mm external diameter tube cooled internally by water. The uncertainty calculation procedure has been tested for the specific case in study considering a wide range of uncertainty intervals in the input variables.

The uncertainty propagation model was able to predict a 95% confidence interval in which the true value was located in 94.5% of the cases analyzed. The uncertainty in the cooling water inlet and outlet temperature measurements constitute a critical factor toward the final uncertainty of the condensation HTC obtained by the Wilson plot method, as well as the minor influence of the uncertainties in the water flow rate and in the vapour temperature measurements. The intermediate results of the uncertainty propagation model reveals that the dominant influence of the water temperature measurements in the final result is due to the large relative uncertainty in the cooling water temperature difference. This aspect gives rise to a large relative uncertainty in the heat transfer rate determination.

The cumulus of results also reveal that the sizing of the experimental set-up, the selecting of operating conditions in the experiment, and the number of data pairs considered to construct the Wilson plot are instrumental in improving the uncertainty in the results obtained by Wilson plot method. On one hand, the enlargement of the tube length and the increment in the logarithmic mean temperature difference contribute to the reduction of the uncertainty in the condensation HTC due to the reduction of the relative uncertainty in the cooling water temperature difference and the heat flow rate. On the other hand, the number of data pairs considered in the Wilson plot plays an important role in the uncertainty in the slope and intercept of the regression line, and thus, in the uncertainty in the final result. Therefore, it should be elevated as much as possible, taking into account the cost and time.

Nomenclature

- A – area, [m^2]
- a – slope of regression line, [–]
- b – intercept of regression line, [–]
- C – fitting constant, [–]
- C_p – specific heat capacity, [Jkg^{-1}K^{-1}]
- d – diameter, [m]
- h – heat transfer coefficient, [Wm^{-2}K^{-1}]
- h^* – variation model of heat transfer coefficient, [Wm^{-2}K^{-1}]
- k – thermal conductivity [Wm^{-1}K^{-1}]
- L – length, [m]
- $\dot{m}$ – mass flow rate (kgs^{-1}]
- Pr – Prandtl number (= $C_p\mu/k$), [–]
- q – heat flow, [W]
- R – thermal resistance, [KW^{-1}]
- Re – Reynolds number (= $4/\dot{m}_{cw}/\mu_{cw}$, $2\dot{m}_c/(\mu_c L_t)$, [–]
- T – temperature, [K], [ºC]
- U – expanded uncertainty, [–]
- u – standard uncertainty, [–]

Greek symbols

- Δ – difference
- μ – dynamic viscosity
- χ^2 – Chi-square function

Subscripts

- c – condensate
- cw – cooling water
- cwi – cooling water inlet
- cwo – cooling water outlet
- i – inner
- j – element j
- lm – logarithmic mean
- o – outer
- ov – overall
- r – relative uncertainty
- t – tube
- v – vapour

Acronyms

CF – coverage factor
UMF – uncertainty magnification factor
UPC – uncertainty percentage contribution

References

[1] Wilson, E. E., A Basis of Rational Design of Heat Transfer Apparatus, *Transactions of ASME, 37* (1915), pp. 47-70
[2] Briggs, D. E., Young, E. H., Modified Wilson Plot Techniques for Obtaining Heat Transfer Correlations for Shell and Tube Heat Exchangers, *Chemical Engineering Progress Symposium Series, 65* (1969), 1, pp. 35-45
[3] Shah, R. K., Assessment of Modified Wilson Plot Techniques for Obtaining Heat Exchanger Design Data, *Proceedings,* 9th International Heat Transfer Conference, Jerusalem, Izrael, 5, 1990, pp. 51-56
[4] Khartabil, H. F., Christensen, R. N., An Improved Scheme for Determining Heat Transfer Correlations for Heat Exchanger Regression Models with Three Unknowns, *Experimental Thermal and Fluid Sciences,* 5 (1992), 6, pp. 808-819
[5] Khartabil, H. F., *et al*., A Modified Wilson Plot Technique for Determining Heat Transfer Correlations, *Proceedings,* UK National Heat Transfer Conference, Columbus, O., USA., 2, 1998, pp. 1331-1357
[6] Fernandez-Seara, J., *et al*., A General Review of the Wilson Plot Method and its Modifications to Determine Convection Coefficients in Heat Exchange Devices, *Applied Thermal Engineering, 27* (2007), 17-18, pp. 2745-2757
[7] Singh, S. K., *et al*., Heat Transfer During Condensation of Steam over a Vertical Grid of Horizontal Integral-Fin Copper Tubes, *Applied Thermal Engineering, 21* (2001), 7, pp. 717-730
[8] Yang, R., Chiang, F. P., An Experimental Heat Transfer Study for Periodically Varying-Curvature Curved-Pipe, *International Journal of Heat and Mass Transfer, 45* (2002), 15, pp. 3199-3204
[9] Rennie, T. J. , Raghavan, V. G. S., Experimental Studies of a Double-Pipe Helical Heat Exchanger, *Experimental Thermal and Fluid Science, 29* (2005), 8, pp. 919-924
[10] Kumar, V., *et al*., Pressure Drop and Heat Transfer Study in Tube-in-Tube Helical Heat Exchanger, *Chemical Engineering Science, 61* (2006), 13, pp. 4403-4416
[11] Xiaowen, Y., Lee, W. L., The Use of Helical Heat Exchangers for Heat Recovery of Domestic Water-Cooled Air-Conditioners, *Energy Conversion and Management, 50* (2009), 2, pp. 240-246
[12] Wjos, K., Tietze, T., Effects of the Temperature Interference on the Results Obtained Using the Wilson Plot Technique, *Heat and Mass Transfer, 33* (1997), 3, pp. 241-245
[13] Styrylska, T. B., Lechowska, A. A., Unified Wilson Plot Method for Determining Heat Transfer Correlations for Heat Exchangers, *Journal of Heat Transfer, 125* (2003), 4, pp. 752-756
[14] Rose, J. W., Heat-Transfer Coefficients, Wilson Plots and Accuracy of Thermal Measurements, *Experimental Thermal and Fluid Science, 28* (2004), 2-3, pp. 77-86
[15] Cheng, B., Tao, W. Q, Experimental Study of R152a Film Condensation on Single Horizontal Smooth Tube and Enhanced Tubes, *ASME Journal of Heat Transfer, 116* (1994), 2, pp. 266-270
[16] ***, Guide to the Expression of the Uncertainty in Measurements, International Organization for Standardization (ISO), 1995
[17] Colburn, A. P., A Method of Correlating Forced Convection Heat Transfer Data and a Comparison with Fluid Friction, *Transactions AIChE, 29* (1933), pp. 174-210
[18] Nusselt, W., Condensation of Steam over Surfaces (in German), *Z. VDI, 60* (1916), pp. 541-546
[19] Bevington, P. R., Robinson, D. K., Data Reduction and Error Analysis for the Physical Sciences, 3rd ed., McGraw-Hill, New York, USA, 2003
[20] Dittus, F. W., Boelter, L. M. K., Heat Transfer in Automobile Radiators of the Tubular Type, *University of California Publications in Engineering, 2*, 1930, pp. 443-461; Reprinted in: *International Communications of Heat and Mass Transfer, 12* (1985), 1, pp. 3-22
[21] Coleman, H. W. Steele, W. G., *Experimentation and Uncertainty Analysis for Engineers*, 2nd ed., John Wiley & Sons, New York, USA, 1998

Paper submitted: July 1, 2011
Paper revised: October 8, 2011
Paper accepted: October 26, 2011